

pubs.acs.org/Macromolecules Article

Surface-Initiated Passing-Through Polymerization on a Rubber Substrate: Supplying Monomer from Swollen Substrates

Sean T. McDermott, Shawn P. Ward, Ngoc Chau H. Vy, Zilu Wang, Mayra Daniela Morales-Acosta, Andrey V. Dobrynin,* and Douglas H. Adamson*



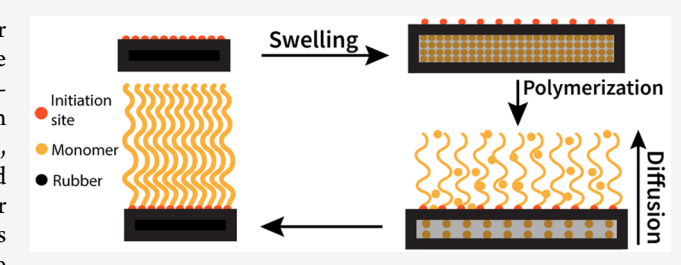
Cite This: Macromolecules 2022, 55, 7265-7272



ACCESS <u>IIII</u> Metr&i Moosre

💷 ArtiRœlceommendat | onsos Support hif nogrmation

ABSTRACT: Passing-through polymerization is a technique for growing surface-initiated polymer brushes where monomers are supplied to the growing chains by diffusing through the initiatorfunctionalized surface. This inverts the monomer concentration gradient relative to conventional grafting-from mechanisms, allowing for the synthesis of thicker and more densely packed brushes. Here we use a combination of coarse-grained computer simulations and experimental techniques to demonstrate how this approach can be implemented, with swellable network-like



substrates supplying monomers to the functionalized surface as they diffuse out of the swollen network. Compared to graftingfrom polymer brushes, this method shows a higher contact angle and a greater brush mass. Additionally, we observed that the passing-through approach could lead to strain-induced crystallization in the brush layer or wrinkling of the brush surface, which we used to estimate the brush thickness. The developed method opens a path for large-scale synthesis of the brush-modified elastic substrates.

INTRODUCTION

Surface-initiated (SI) polymer brushes have drawn considerable attention due to their ability to alter the lubricating, 1,2 wetting,³ antifouling,⁴ and adhesive⁵ properties of surfaces as well as their application for stimuli-responsive substrates.⁶ These unique properties are reflections of the chain conformations in a brush.^{7,8} In particular, at high grafting densities, the strong steric repulsion between neighboring chains forces their extension, thus creating a protective brush layer of stretched chains above the surface. $^{9-11}$

SI brushes are synthesized by a variety of polymerization mechanisms, including nitroxide-mediated polymerization (NMP), 12 reversible addition-fragmentation transfer (RAFT), 13 and most commonly atom transfer radical polymerization (ATRP),14 which has an advantage due to its tolerance of a broad range of solvents and reaction conditions. 15,16 These mechanisms are then employed to create SI brushes by using one of two main approaches: grafting-to and grafting-from. In the grafting-to approach, polymers are first grown in solution then attached to a surface. An advantage of this approach is that the chains are produced before they are attached, allowing for their detailed characterization. However, a disadvantage is that the attachment of a chain sterically impedes other chains from connecting near it, as the grafted chains shield neighboring attachment sites. The result is lower grafting density and no chain extension.¹

Grafting-from, in contrast, initiates polymerization directly from the surface, which leads to much higher grafting densities than in the grafting-to systems. Although this method is typically preferred, it suffers from chain characterization challenges and concentration gradient issues during the brush polymerization process. As the chains grow, a monomer deficient region forms close to the surface. 18-23 This results in an environment where the longer chains that reach further into the surrounding solution encounter a greater monomer concentration and grow faster than the shorter ones. The overall effect is a significant increase in D. A large value of D means that the longer chains extend above the shorter chains, adopting less extended conformations. This means that the surface properties result from random coil polymer chains rather than extended polymer brushes.²⁴

We have introduced a passing-through SI polymerization method to address the monomer concentration gradient limitation associated with grafting-from approaches. 25,26 Passing-through inverts the monomer concentration gradient by supplying the monomer through a permeable surface on which the initiator is attached. As monomer diffuses through the substrate, the concentration of the monomer is highest near the surface, inverting the concentration gradient seen in

Received: April 4, 2022 Revised: July 11, 2022 Published: August 5, 2022





Scheme 1. Outline of the Reaction Approach for the Functionalization of SBR, Followed by Passing-Through Polymerization

grafting-from approaches. This leads to a more uniform brush due to the shorter chains seeing a higher monomer concentration than the longer chains. Combining this approach with monomer swollen elastic networks, styrene—butadiene rubber (SBR), provides a synergy that results in highly dense SI brushes not possible with current grafting-from techniques. The monomer is supplied to the SI brushes from the underlying network, meaning that the chain growth occurs concurrently with substrate compression. Using both experimental and computational approaches, we demonstrate the new approach's effect on the surface properties of the elastic network and propose a mechanism of chain growth as the swollen network shrinks.

MATERIALS AND METHODS

Materials. Hydrochloric acid (HCl) (ACS reagent, 37%), sodium hydroxide (NaOH) (Fisher Chemicals, pellets), toluene (Fisher Chemicals, certified ACS), bromine liquid (Alfa Aesar, 99.5%), hexane (Fisher Chemicals, certified ACS), argon (Airgas), 2-bromo-2methylpropanoic acid (Alfa Aesar 98%), triethylamine (TCI America, 99%), acetone (Fisher Chemicals), copper(II) bromide (CuBr₂) (Acros Organics, 99+%), 1,1,4,7,7-pentamethyldiethylenetriamine (PMDTA) (98+%, Acros Organics), borane-dimethyl sulfide complex (BH₃-SMe₃) (Alfa Aesar, 94%), ethanol (Fisher chemical, reagent grade), hydrogen peroxide (Sigma-Aldrich, 30 wt %), chloroform (Fisher Chemicals), and 2-bromoisobutyryl bromide (BIBB) (Acros Organic, 98%) were used as received. Copper(I) bromide (CuBr) (Alfa Aesar, 99%) was purified by using a known procedure involving multiple acid washes.²⁷ Styrene (Sigma-Aldrich, >99%) and tert-butyl acrylate (Sigma-Aldrich, 98%) were passed through a packed column to remove the inhibitor (Sigma-Aldrich, 311340 for styrene, and Sigma-Aldrich, 311332 for tert-butyl acrylate) before use. In addition, styrene-butadiene rubber (SBR) (McMaster-Carr, abrasion-resistant rubber) was treated prior to use to remove impurities as described below.

Extraction of Impurities from the Rubber. The SBR was washed with deionized water (DI water) and patted dry. ²⁸ It was then submerged in 100 mL of DI water and boiled for 1 h. It was then removed, washed with DI water, and dried. This process was repeated with 1 M HCl and 1 M NaOH, with the SBR washed with copious amounts of water between each extraction solvent. Next, it was placed into a reactor and refluxed with 100 mL of toluene for 1 h. The sample was then washed acetone and DI water and air-dried for 24 h as per the literature procedure. ²⁸

Bromination of the Rubber Sheets. A round-bottom flask was charged with 1.8 mL of liquid bromine and 100 mL of hexane and stirred until homogeneous. The flask was then purged with argon for 30 min, after which 5 g of extracted SBR was added and stirred for 3 h at room temperature. Successful bromination was indicated by a color change of the solution from dark red to clear. The brominated SBR was then washed with DI water and dried under vacuum for 24 h.

Initiator Functionalization. Initiator attachment was done in excess 2-bromo-2-methylpropanoic acid. In a typical reaction, 9 g of 2-bromo-2-methylpropanoic acid was dissolved in 200 mL of toluene, followed by the addition of 25 mL of dried triethylamine. The brominated SBR was then added to the solution and refluxed for 24 h while being stirred. This was then washed with copious amounts of acetone, toluene, and DI water and vacuum-dried for 24 h.

Passing-Through Polymerization. The initiator-attached SBR was placed in a closed container with excess tert-butyl acrylate (t-BA) and allowed to sit for 48 h until it had swollen to maximum capacity; that is, no further change in volume was observed. Then a roundbottom flask was charged with 200 mL of DI water, 42 mg of CuBr, 7 mg of CuBr $_2$ and 67 μ L of PMDTA and allowed to stir for 1 h or until the solution was homogeneous. Next, the solution was degassed by high vacuum, backfilled with argon, and sealed. The swollen SBR was then transferred to an empty round-bottom flask, degassed, and backfilled with argon by using the same procedure. The SBR was then quickly transferred to the reaction flask under a constant stream of argon and sealed. An argon-filled balloon was used to maintain an inert atmosphere throughout the polymerization. The reaction flask was then placed in an oil bath at 60 °C and allowed to react overnight. The supernatant was then filtered off, and the SBR was washed with copious amounts of acetone, water, and 0.1 N HCl to remove any remaining homopolymer or copper.

Hydroboration and Initiator Attachment. A round-bottom flask was charged with 100 mL of hexane, a 1 cm by 1 cm rubber piece, and 0.15 mL of BH_3 – SMe_3 and allowed to stir for 48 h at room temperature. The reaction mixture was then cooled to 0 °C in an ice bath. Next, 11.2 mL of ethanol, 4.06 mL of 4 M NaOH, and 0.676 mL of hydrogen peroxide were added and stirred for 2 h. After this, 300 mL of water was added to terminate the reaction. ²⁹ Initiator attachment was accomplished by placing the rubber piece in a 50 mL solution of BIBB (0.2 mL) and chloroform and then stirring for 2 h at room temperature. The swelling process and polymerization followed the same procedure as previously described, with styrene being used instead of t-BA, and at a temperature of 70 °C for the oil bath during the polymerization.

Characterization. ATR-FTIR spectra were obtained by using a Nicolet Magna 560 instrument. The brush mass was determined by using a TA Instruments TGA Q-500. The samples were heated at a rate of 10 °C/min in a nitrogen environment. The contact angle was determined by using water on a Dataphysics OCA 20 contact angle system and accompanying SCA software for image analysis and data recording. Optical images were taken by using a Leica M-125. SEM images were captured on a FEI NovaSEM 450, and EDS images were taken by using an Oxford AZecEnergy microanalysis system with X-Max 80 silicon drift detector attachment. The surface morphology of the rubber was visualized by using an atomic force microscope (Asylum Research MFP-3D). Samples were first mounted onto glass slides with double-sided tape. Imaging was performed in tapping mode by using silicon tips (Asylum Probe, AC-160, spring constant ~26 N/m, tip radius of 7 nm, resonance frequency ~300 kHz). Scans sizes between 2 \times 2 μ m² and 10 \times 10 μ m² were acquired at line rates of 1 Hz, with typical set point and feedback gain settings optimized

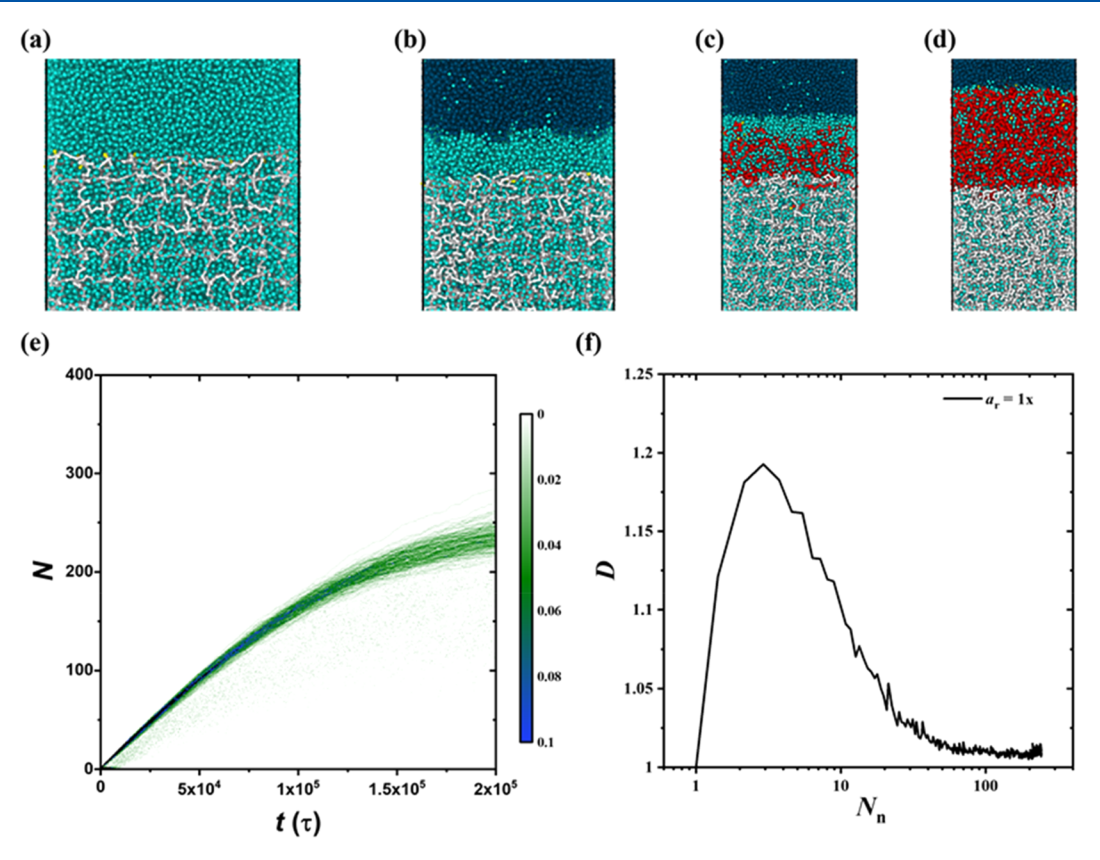


Figure 1. Simulation steps of brush polymerization on the surface of a swollen network in coarse-grained molecular dynamics simulations: (a) Polymer network swollen in monomeric liquid. (b) Polymer network swollen with monomers placed in a poor solvent for monomers and network strands. (c, d) Brush polymerization. (e) Evolution of the distribution of chain degree of polymerization N in brush layer during polymerization. (f) Brush dispersity index as a function of the number-average degree of polymerization. a_r is a numerical coefficient describing probability of chain polymerization reaction as explained in the Supporting Information.

for surface tracking. Two-dimensional wide-angle X-ray scattering (WAXS) frames were acquired in transmission mode by using an Oxford Xcalibur diffractometer equipped with a CCD detector and Cu K α radiation (λ = 1.54184 Å) operated at 45 kV and 45 mA. The measurements were performed at room temperature. The one-dimensional WAXS patterns were obtained by azimuthal integration around the beam center.

■ RESULTS AND DISCUSSION

Because styrene—butadiene rubber (SBR) does not contain hydroxyl groups that allow attachment of the BIBB initiator by reaction with acid bromides as is commonly done, we investigated both the hydroxylation and bromination of the surface as described in the Materials and Methods section. Hydroxylation allowed attachment of the initiator by acid bromides, while bromination allowed the attachment of the initiator by an $\rm S_{\rm N}2$ mechanism through the carboxylic acid of 2-bromo-2-methylpropanoic acid. We found that bromination was more straightforward than hydroxylation, so this was our method of choice, as illustrated in Scheme 1.

The initiator-functionalized SBR was then swollen in a monomer such that the swelling capacity of the rubber limited the total monomer added to the system. We then placed the monomer-swollen SBR in an aqueous solution containing ATRP activator/deactivator reagents, and the SI brushes were grown as the monomer diffused out of the rubber. Our previous work has shown that this approach leads to thicker polymer brushes with smaller values of \mathcal{D} as compared to grafting-from approaches. ^{25,26} In the current investigation, we

ultimately used water as the surrounding solvent due to its lower volatility and environmentally friendly nature as compared to acetone. Additionally, the monomer has minimal solubility in water, keeping the monomer at the surface.

Figure 1 presents results of our coarse-grained computer simulations of the main steps of brush growth from the initiator functionalized surface of the swellable network-like substrate. The process begins with swelling the surfacefunctionalized network with monomer, followed by placement of the swollen network in a poor solvent for the monomer and network strands (water in the current method implementation). In addition to inverting the monomer concentration gradient, the passing-through brush growth has the additional feature of the swollen substrate compressing during the brush polymerization as the monomers diffuse out. This increases the brush grafting density and chain stretching during brush growth. This behavior is known for brush layers on responsive substrates.³⁰ Furthermore, the dispersity of the growing chains in the brush layer approached unity at the later stages of the polymerization process when almost all monomers were consumed. The main features of the time evolution of the chain distribution are similar to those observed for brush growth on the surface of monomer permeable membranes.²⁵ Confirming the feasibility and mechanism of the approach by molecular dynamics simulations in Figure 1, with more detailed information about the simulation contained in Figures S1 and S2, we focus on the practical implementation of the approach and the properties of the brush layer.

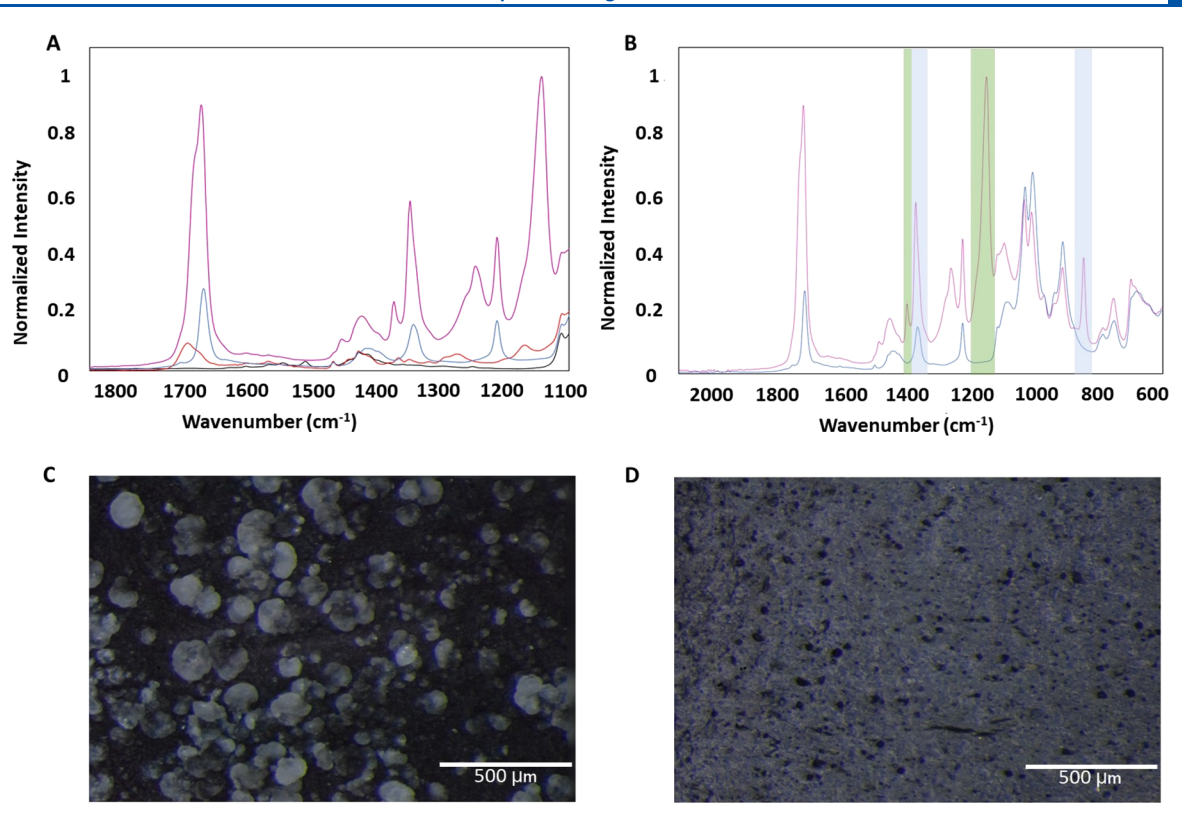


Figure 2. (A) ATR-FTIR of pristine rubber (black), initiator attached (red), passing-through grown brush (pink), and grafting-from grown brush (blue). The inset highlights the carbonyl stretch, which appears after initiator attachment, and shifts after polymerization. (B) ATR-FTIR spectra of the passing-through (pink) and the grafting-from (blue), with key peaks highlighted. The blue highlighted region indicates amorphous polymer, while the green highlighted region indicates crystalline polymer. Images C and D are the surfaces of grafted rubber viewed under an optical microscope, C being the passing-through sample and D being the grafting-from sample.

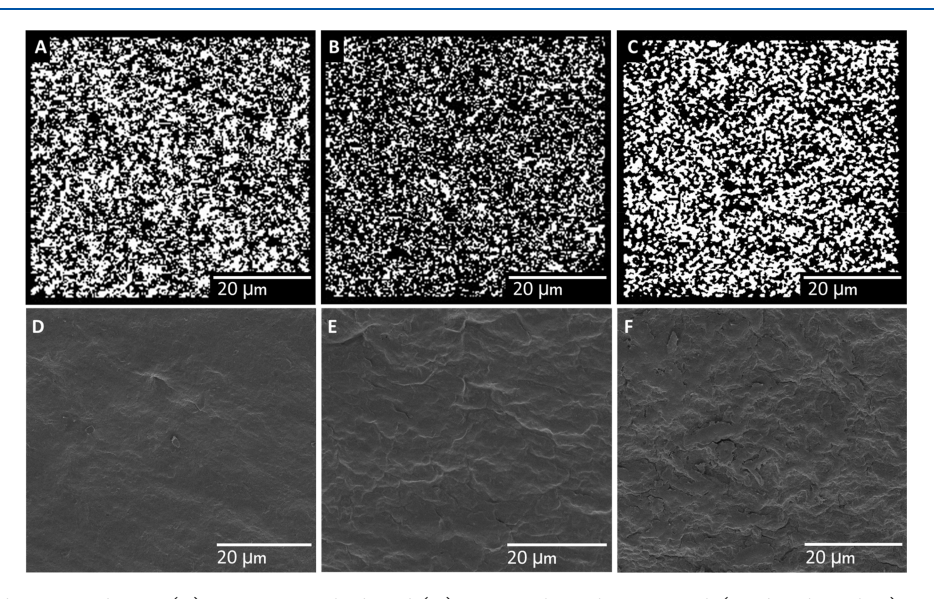


Figure 3. EDS of (A) brominated SBR, (B) initiator-attached, and (C) passing-through grown poly(*tert*-butyl acrylate). SEM of (D) brominated SBR, (E) initiator-attached, and (F) passing-through. The EDS of each shows the Br (L) peak; these images were processed through ImageJ to convert them to black and white, where white indicates Br atoms on the surface. The EDS images were taken at the same magnification as the SEM images and are in the same spot as the image below them.

ATR-FTIR was used to characterize the rubber at each stage of the surface functionalization process. Pristine surface-functionalized SBR brushes grown with our passing-through approach and a grafting-from control are shown in Figure 2A, with a complete overlay presented in Figure S3. Figure 2A shows successful initiator attachment and polymerization as

indicated by the presence and intensity of the carbonyl peak at \sim 1735 cm⁻¹ (C=O stretching), which was initially absent in the pristine and Br-treated SBR. We observed the carbonyl peak only after initiator attachment. Post-polymerization, the intensity of the peak increased significantly, with a new peak emerging at \sim 1365 cm⁻¹ corresponding to C-H bending from

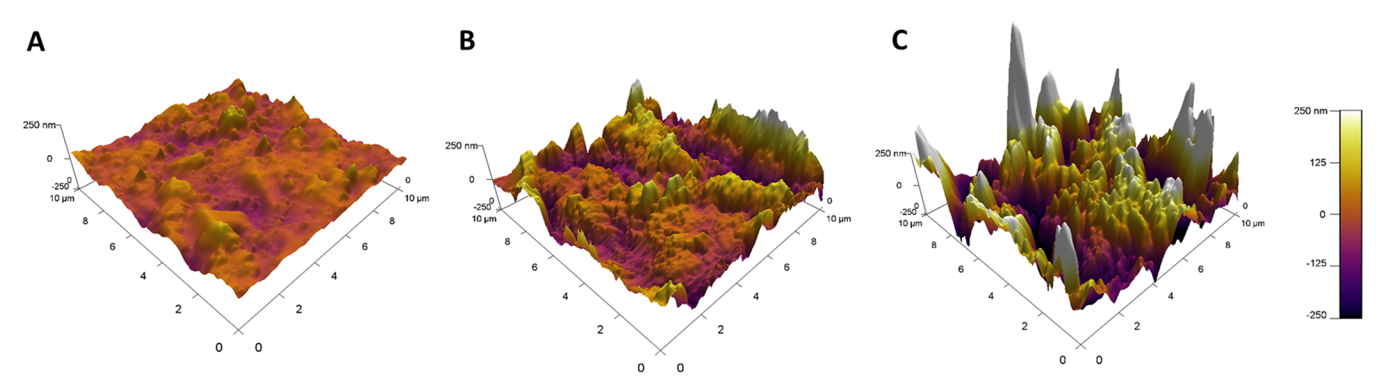


Figure 4. AFM of a 10 by $10 \mu m^2$ surface section and vertical scale runs between -250 and 250 nm: (A) pristine SBR, (B) grafting-from, and (C) passing-through grown polymer (AFM comparing the functionalized to the grown samples can be seen in Figure S8).

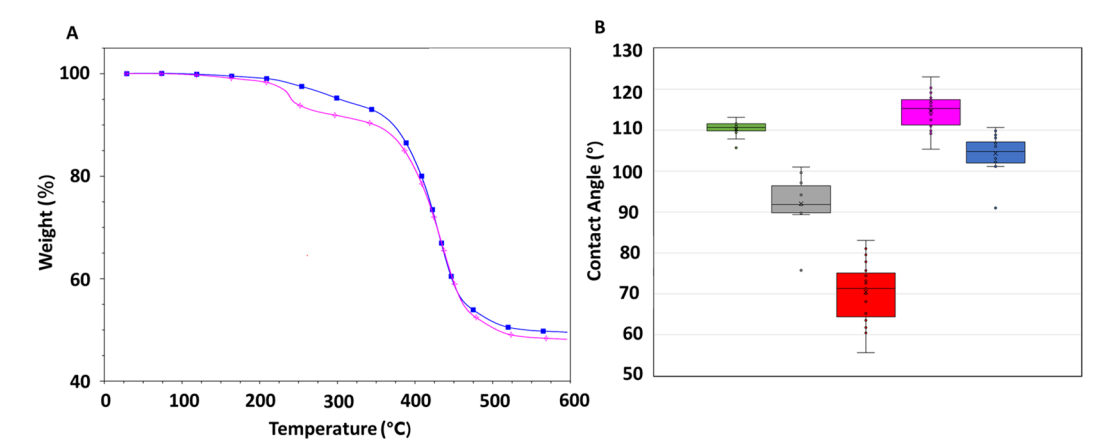


Figure 5. TGA of brush modified SBR (thermal degradation of each step of the functionalization can be seen in Figure S9) (A) passing-through (pink) and grafting-from (blue). (B) Contact angle of pristine SBR (green), brominated (gray), initiator-attached (red), passing-through (pink), and grafting-from (blue).

the *tert*-butyl group, confirming the presence of P(t-BA) on the surface. These changes in peak position and intensity were present in all surface-grown systems, though the effect was less dramatic in the grafting-from samples. The intensity difference indicates a greater mass of brush polymer in the passing-through brush than the grafting-from brush. To ensure that growth of the brushes was occurring solely on the surface of the rubber, an initiator attached sample was cut down the middle for FTIR analysis. It was found there was no initiator on the interior of the rubber, as shown in Figure S5. 31

Despite similarities in the FTIR of the grafting-from and passing-through systems, we observed differences. As emphasized in Figure 2B, peaks at ~1365 and ~844 cm⁻¹ indicate the presence of amorphous P(t-BA), while peaks at \sim 1392 and ~ 1147 cm⁻¹ are indicative of crystalline P(t-BA).³² These crystalline regions take the shape of spherulites on the surface of the rubber, as seen in Figure 2C. This crystallinity was also studied by using XRD, showing crystal structure was present after the polymer chains were grown via the passing-though method, as seen in Figure S4. This crystalline region in the passing-through sample resulted from the close packing of brushes and was absent in the grafting-from control. At the beginning of the reaction, the polymer chains are lower molecular weight and more spread out due to the swollen substrate. As monomer diffuses out and the chains increase in MW, the substrate shrinks, forcing the chains closer together. Crystallinity is induced on the surface in these high graftingdensity regimes, while the amorphous regions represent

slightly extended chains with lower grafting densities. This can be seen in Figure S6.

While FTIR is valuable for proving surface functionalization and brush growth, it says little about the density or uniformity of the initiator at the surface. For this, we employed SEM and energy-dispersive X-ray spectroscopy (EDS) to image the bromine on the SBR surface (Figure 3A), the initiatorfunctionalized SBR (Figure 3B), and the brush-modified SBR (Figure 3C).³³ EDS mapping of bromine shows uniform surface coverage with Br irrespective of surface roughness. Image analysis using pixel counting was also employed. The weight precent of bromine for the brominated, initiatorattached, and passing-through sample is shown in Figure S7. SEM of the functionalized SBR surfaces revealed that the surface remained smooth after bromination but began to roughen after initiator attachment (Figure 3D). This surface roughening shown in Figure 3E is likely due to the removal of toluene. In contrast, the significant increase in surface roughness, as seen in Figure 3F, resulted from the presence of surface-initiated polymer brushes.

To better characterize the observed changes in the surface morphology of the SBR, we used AFM, with results shown in Figure 4. While the pristine SBR surface is not atomically smooth (Figure 4A), it is clearly smoother than grafting-from (Figure 4B) or passing-through surfaces (Figure 4C). Although both the grafting-from and passing-through surfaces have attached polymer chains, the passing-through polymer chains have a thickness of 188 nm, and the grafting from sample has a

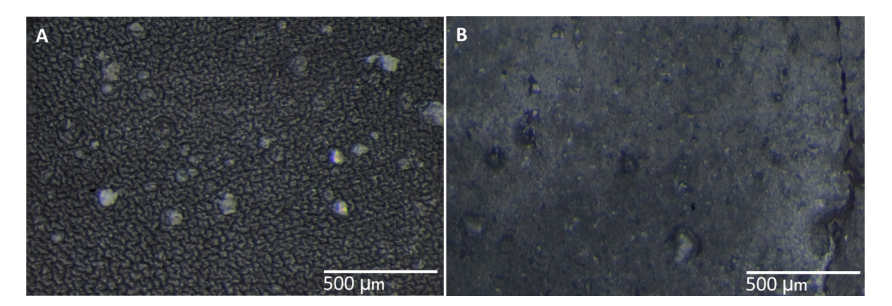


Figure 6. (A) Optical image of passing-through grown PS brush surface. (B) The same sample seen in image A after cleavage of the PS brushes from the surface.

brush thickness of 144 nm. We attributed this difference to different brush growth mechanisms. The passing-through mechanism's inverted monomer concentration gradient results in a significantly greater polymerization rate, leading to a thicker and more complete layer of brushes on the SBR surface. This, in turn, results in greater chain extension and reduced chain mobility, leading to the crystallinity observed in Figure 2.

This thicker brush layer means the passing-through sample should also have a greater P(t-BA) mass on the surface than the grafting-from sample. Thermal gravimetric analysis (TGA) of the grafting-from versus passing-through samples (Figure 5A) indicated that the total polymer mass was greater in the passing-through sample; more specifically, the observed mass loss occurring at 225 °C corresponded to degradation of P(t-BA). The grafting-from sample showed a mass loss of 4.99% in this region, while the passing-through sample showed a mass loss of 7.54%. When we compared the mass loss in the P(t-BA) region to the residue remaining, the passing through sample showed a 5.7% greater mass loss, indicating the passing-through approach produced 1.5× the SI brush polymer mass compared to the grafting-from control. This agrees with the AFM images seen in Figure 4.

Contact angle measurements (Figure 5B) are further evidence of the passing-through approach's greater surface coverage. The bromine-functionalized surface and the initiator functionalized surface both showed a decrease in contact angle compared to the pristine rubber, as both increased the hydrophilicity of the surface. Attachment of P(t-BA) brushes significantly increased the contact angle of the rubber. This increase in hydrophobicity resulted from the polymer coating, but more interesting was the observation that the contact angle for the passing-through sample was greater than the grafting-from sample. This difference in contact angle indicated that the passing-through brushes more completely coated the SBR surface than the grafting-from brushes.

Although the bromination approach to functionalizing the SBR was convenient and effective, other functionalization approaches, such as hydroboration, are possible. While this approach was more time-consuming and challenging to scale, it did not require heating, possibly allowing for more temperature sensitive substrates to be used. Figure 6A shows a passing-through grown PS brush prepared via the hydroboration approach. Figure 6B shows the surface after cleaving the brush by using 1 M HCl. Of note is that the wrinkles that covered the SBR surface in Figure 6A disappear when the brushes are cleaved from the surface.

This wrinkling phenomenon was previously reported by Huang et al. for poly(hydroxyethyl methacrylate) (PHEMA) brushes grown on PDMS and was used to determine the height of their SI polymer brushes. They found that when responding to thermal influences, the PHEMA brushes would transition to a glassy state before the PDMS substrate became glassy, causing the PHEMA to contract and form unoriented wrinkles as the temperature dropped below its $T_{\rm g}$. They also observed that compression could drive the formation of wrinkles, leading to wrinkling orientation in the direction of the force. However, in our passing-through system, the wrinkling was caused via the thermal mechanism rather than compression as no orientation of the wrinkles was observed, as seen in Figure 6A.

This wrinkling provided an avenue to characterize the SI polymer brushes. Even with well-controlled polymerization techniques, brush systems produce a low mass of polymer, which can make polymer characterization difficult for some systems. An approach often used in the literature to address this challenge is to add a sacrificial initiator to the polymerization solution. An assumption is then made that the polymer grown in solution is representative of the polymer grown from the surface, providing an approximation of the surface-attached polymer molecular weight for grafting density calculations. However, this assumption is known to be problematic and likely gives incorrect values of brush polymer MW. ^{24,39–41}

Huang et al. used wrinkling to determine the brush height of their material using eq 1

$$h_{\rm b} = \frac{\lambda}{2\pi} \left(\frac{\overline{E}_{\rm b}}{3\overline{E}_{\rm s}} \right)^{-1/3} \tag{1}$$

where h_b is the brush height and \overline{E}_b and \overline{E}_s are the plane-strain modulus of the brushes and the substrate, respectively. These are defined as $E/(1-v^2)$, where E is Young's modulus. The wavelength (λ) refers to the distance between ridges in the wrinkles. In our system, we obtained this value by measuring the distance between the wrinkles using image analysis on ImageJ. The Young's modulus of the substrate was obtained from the manufacturer's specifications. For the brushes' elastic modulus, we used 0.6 GPa, as determined by Julthongpiput et al. when studying the elastic modulus of PS and P(t-BA)brushes on a silicon substrate. 42 Using these values, we calculated the brush height for our passing-through SI brush shown in Figure 6A to be 310 nm. This value is similar to the 188 nm brush height estimated by AFM in Figure 4 for the P(t-BA) brushes grown by passing-through; we believe the difference comes from the different monomers used. Our AFM images were taken on P(t-BA) grown brushes, while the wrinkling occurred only with the PS grown brushes.

CONCLUSIONS

Supplying monomer to a surface-initiated brush by diffusing monomer from within the substrate using a passing-through mechanism inverts the monomer gradient in the system, increasing the monomer concentration at the surface relative to the monomer concentration further from the growing chains. We showed that the combination of an initially swollen surface and a passing-through-brush growth mechanism increased the thickness and mass of the surface-initiated brushes while keeping the surface chain coverage uniform. Compared to the commonly used grafting-from approach to surface-initiated chain growth, this passing-through approach on swollen substrates generated surfaces that were more hydrophobic and contained 1.5 times more polymer brush mass than grafting-from controls. Chain crystallization and dry substrate wrinkling were also observed with the passing-through approach but not with grafting-from controls. Crystallinity appeared to be induced by the increased grafting density and height of P(t-BA) brushes and was confirmed by FTIR and optical microscopy. The wrinkling seen in PS brushes resulted from thermal forces and was reported by others to require a high grafting density to form. These wrinkles enabled us to estimate the brush height in our system to be 310 nm. Applying the passing-through mechanism for surface-initiated brush growth on swollen substrates produces thicker and more dense brushes than was previously possible by traditional approaches.

Furthermore, the presented approach creates opportunities for large-scale synthesis of the brush-coated responsive substrates that combine the properties of the brushes and polymer networks. The developed approach is flexible in terms of monomer selection and could be used for the polymerization of brush layers made of multiblock copolymers. Such surfaces could find applications as adhesives, lubricating coatings, and multifunctional substrates whose properties could be judicially controlled during brush synthesis. We hope that this paper will inspire future research in this direction.

ASSOCIATED CONTENT

Supporting Information

The Supporting Information is available free of charge at https://pubs.acs.org/doi/10.1021/acs.macromol.2c00685.

Detailed information about the computational studies, such as a simulation box, interaction parameters, effect of mesh size and dispersity index of chains as a function of rate of monomer addition; FTIR of all controls and the interior of the rubber; optical images that show the effect of freely accessible activator; surface EDS table; AFM of the surface of the initiator attached SBR; TGA of all steps of the functionalization (PDF)

■ AUTHOR INFORMATION

Corresponding Authors

Andrey V. Dobrynin — Department of Chemistry, University of North Carolina, Chapel Hill, North Carolina 27599, United States; orcid.org/0000-0002-6484-7409; Email: avd@email.unc.edu

Douglas H. Adamson – Polymer Program, Institute of Materials Science and Department of Chemistry, University of Connecticut, Storrs, Connecticut 06269, United States; orcid.org/0000-0002-7719-9287; Email: douglas.adamson@uconn.edu

Authors

Sean T. McDermott — Polymer Program, Institute of Materials Science, University of Connecticut, Storrs, Connecticut 06269, United States; orcid.org/0000-0002-0669-9604

Shawn P. Ward — Department of Chemistry, University of Connecticut, Storrs, Connecticut 06269, United States;
orcid.org/0000-0002-4992-2925

Ngoc Chau H. Vy — Polymer Program, Institute of Materials Science, University of Connecticut, Storrs, Connecticut 06269, United States; orcid.org/0000-0001-9007-4705

Zilu Wang — Department of Chemistry, University of North Carolina, Chapel Hill, North Carolina 27599, United States; occid.org/0000-0002-5957-8064

Mayra Daniela Morales-Acosta — Polymer Program, Institute of Materials Science, University of Connecticut, Storrs, Connecticut 06269, United States

Complete contact information is available at: https://pubs.acs.org/10.1021/acs.macromol.2c00685

Notes

The authors declare no competing financial interest.

ACKNOWLEDGMENTS

The authors thank the Department of Education for the Graduate Assistance in Areas of National Need (GAANN) fellowship awards P200A150330 and P200A180065 and the National Science Foundation award CHE2004072 for funding this work.

REFERENCES

- (1) Bahrami, M.; Le Houérou, V.; Rühe, J. Lubrication of Surfaces Covered by Surface-Attached Hydrogel Layers. *Tribol. Int.* **2020**, *149* (2020), 105637.
- (2) Zhang, K.; Yan, W.; Simic, R.; Benetti, E. M.; Spencer, N. D. Versatile Surface Modification of Hydrogels by Surface-Initiated, Cu0-Mediated Controlled Radical Polymerization. *ACS Appl. Mater. Interfaces* **2020**, *12* (5), *6761–6767*.
- (3) Sui, X.; Zapotoczny, S.; Benetti, E. M.; Schön, P.; Vancso, G. J. Characterization and Molecular Engineering of Surface-Grafted Polymer Brushes across the Length Scales by Atomic Force Microscopy. *J. Mater. Chem.* **2010**, 20 (24), 4981–4993.
- (4) Ye, Q.; He, B.; Zhang, Y.; Zhang, J.; Liu, S.; Zhou, F. Grafting Robust Thick Zwitterionic Polymer Brushes via Subsurface-Initiated Ring-Opening Metathesis Polymerization for Antimicrobial and Anti-Biofouling. ACS Appl. Mater. Interfaces 2019, 11 (42), 39171–39178.
- (5) Bhairamadgi, N. S.; Pujari, S. P.; Leermakers, F. A. M.; Van Rijn, C. J. M.; Zuilhof, H. Adhesion and Friction Properties of Polymer Brushes: Fluoro versus Nonfluoro Polymer Brushes at Varying Thickness. *Langmuir* **2014**, *30* (8), 2068–2076.
- (6) Motornov, M.; Sheparovych, R.; Lupitskyy, R.; MacWilliams, E.; Hoy, O.; Luzinov, I.; Minko, S. Stimuli-Responsive Colloidal Systems from Mixed Brush-Coated Nanoparticles. *Adv. Funct. Mater.* **2007**, *17* (14), 2307–2314.
- (7) Milner, S. T. Polymer Brushes. Science (80-.) 1991, 251 (4996), 905–914.
- (8) Galvin, C. J.; Genzer, J. Applications of Surface-Grafted Macromolecules Derived from Post-Polymerization Modification Reactions. *Prog. Polym. Sci.* **2012**, *37* (7), 871–906.
- (9) Brittain, W. J.; Minko, S. A Structural Definition of Polymer Brushes. J. Polym. Sci. Part A Polym. Chem. 2007, 45 (16), 3505–3512.

- (10) Yan, W.; Ramakrishna, S. N.; Spencer, N. D.; Benetti, E. M. Brushes, Graft Copolymers, or Bottlebrushes? The Effect of Polymer Architecture on the Nanotribological Properties of Grafted-from Assemblies. *Langmuir* **2019**, 35 (35), 11255–11264.
- (11) Milner, S. T. Polymer Brushes. Science (80-.) 1991, 251 (4996), 905-914.
- (12) Ignatova, M.; Voccia, S.; Gilbert, B.; Markova, N.; Mercuri, P. S.; Galleni, M.; Sciannamea, V.; Lenoir, S.; Cossement, D.; Gouttebaron, R.; Jérôme, R.; Jérôme, C. Synthesis of Copolymer Brushes Endowed with Adhesion to Stainless Steel Surfaces and Antibacterial Properties by Controlled Nitroxide-Mediated Radical Polymerization. *Langmuir* **2004**, *20* (24), 10718–10726.
- (13) Baum, M.; Brittain, W. J. Synthesis of Polymer Brushes on Silicate Substrates via Reversible Addition Fragmentation Chain Transfer Technique. *Macromolecules* **2002**, 35 (3), 610–615.
- (14) Wang, J. S.; Matyjaszewski, K. Controlled/"Living" Radical Polymerization. Atom Transfer Radical Polymerization in the Presence of Transition-Metal Complexes. J. Am. Chem. Soc. 1995, 117 (20), 5614–5615.
- (15) Chen, W. L.; Cordero, R.; Tran, H.; Ober, C. K. 50th Anniversary Perspective: Polymer Brushes: Novel Surfaces for Future Materials. *Macromolecules* **2017**, *50* (11), 4089–4113.
- (16) Zoppe, J. O.; Ataman, N. C.; Mocny, P.; Wang, J.; Moraes, J.; Klok, H. A. Surface-Initiated Controlled Radical Polymerization: State-of-the-Art, Opportunities, and Challenges in Surface and Interface Engineering with Polymer Brushes. *Chem. Rev.* **2017**, *117* (3), 1105–1318.
- (17) Zdyrko, B.; Luzinov, I. Polymer Brushes by the "Grafting to" Method. *Macromol. Rapid Commun.* **2011**, 32 (12), 859–869.
- (18) Zhao, B.; Brittain, W. J. Synthesis of Tethered Polystyrene-Block-Poly(Methyl Methacrylate) Monolayer on a Silicate Substrate by Sequential Carbocationic Polymerization and Atom Transfer Radical Polymerization [15]. *J. Am. Chem. Soc.* **1999**, *121* (14), 3557–3558.
- (19) Jordan, R.; Ulman, A.; Kang, J. F.; Rafailovich, M. H.; Sokolov, J. Surface-Initiated Anionic Polymerization of Styrene by Means of Self Assembled Monolayers. *J. Am. Chem. Soc.* **1999**, *121* (5), 1016–1022.
- (20) Kim, J. B.; Bruening, M. L.; Baker, G. L. Surface-Initiated Atom Transfer Radical Polymerization on Gold at Ambient Temperature [13]. *J. Am. Chem. Soc.* **2000**, *122* (31), 7616–7617.
- (21) Jordan, R.; Ulman, A. Surface Initiated Living Cationic Polymerization of 2-Oxazolines. *J. Am. Chem. Soc.* **1998**, 120 (2), 243–247.
- (22) Demirci, S.; Kinali-Demirci, S.; VanVeller, B. Controlled Supramolecular Complexation of Cyclodextrin-Functionalized Polymeric Ionic Liquid Brushes. *ACS Appl. Polym. Mater.* **2020**, 2 (2), 751–757.
- (23) Zeng, Y.; Xie, L.; Chi, F.; Liu, D.; Wu, H.; Pan, N.; Sun, G. Controlled Growth of Ultra-Thick Polymer Brushes via Surface-Initiated Atom Transfer Radical Polymerization with Active Polymers as Initiators. *Macromol. Rapid Commun.* **2019**, *40* (13), 1–5.
- (24) Martinez, A. P.; Carrillo, J. Y.; Dobrynin, A. V.; Adamson, D. H. Distribution of Chains in Polymer Brushes Produced by a "Grafting From" Mechanism. *Macromolecules* **2016**, 49 (2), 547–553.
- (25) Mohammadi Sejoubsari, R.; Martinez, A. P.; Kutes, Y.; Wang, Z.; Dobrynin, A. V.; Adamson, D. H. Grafting-Through": Growing Polymer Brushes by Supplying Monomers through the Surface. *Macromolecules* **2016**, 49 (7), 2477–2483.
- (26) Vy, N. C. H.; Liyanage, C. D.; Williams, R. M. L.; Fang, J. M.; Kerns, P. M.; Schniepp, H. C.; Adamson, D. H. Surface-Initiated Passing-through Zwitterionic Polymer Brushes for Salt-Selective and Antifouling Materials. *Macromolecules* **2020**, 53 (22), 10278–10288.
- (27) Opsteen, J. A.; Brinkhuis, R. P.; Teeuwen, R. L. M.; Löwik, D. W. P. M.; Van Hest, J. C. M. Clickable" Polymersomes. *Chem. Commun.* **2007**, 7345 (30), 3136–3138.
- (28) Rungrodnimitchai, S.; Kotatha, D. Chemically Modified Ground Tire Rubber as Fluoride Ions Adsorbents. *Chem. Eng. J.* **2015**, 282, 161–169.

- (29) Li, J.; Sung, S.; Tian, J.; Bergbreiter, D. E. Polyisobutylene Supports A Non-Polar Hydrocarbon Analog of PEG Supports. *Tetrahedron* **2005**, *61* (51), 12081–12092.
- (30) Wu, T.; Efimenko, K.; Genzer, J. Preparing High-Density Polymer Brushes by Mechanically Assisted Polymer Assembly. *Macromolecules* **2001**, 34 (4), 684–686.
- (31) Xie, Y.; Moreno, N.; Calo, V. M.; Cheng, H.; Hong, P. Y.; Sougrat, R.; Behzad, A. R.; Tayouo, R.; Nunes, S. P. Synthesis of Highly Porous Poly(: Tert -Butyl Acrylate)- b -Polysulfone- b -Poly(Tert -Butyl Acrylate) Asymmetric Membranes. *Polym. Chem.* **2016**, 7 (18), 3076–3089.
- (32) Kawasaki, A.; Furukawa, J.; Tsuruta, T.; Wasai, G.; Makimoto, T. Infrared Spectra of Poly(Butyl Acrylates). *Macromol. Chem.* **1961**, 49 (1), 76–111.
- (33) Bandodkar, A. J.; You, J. M.; Kim, N. H.; Gu, Y.; Kumar, R.; Mohan, A. M. V.; Kurniawan, J.; Imani, S.; Nakagawa, T.; Parish, B.; Parthasarathy, M.; Mercier, P. P.; Xu, S.; Wang, J. Soft, Stretchable, High Power Density Electronic Skin-Based Biofuel Cells for Scavenging Energy from Human Sweat. *Energy Environ. Sci.* 2017, 10 (7), 1581–1589.
- (34) Saikia, B. J.; Dolui, S. K. Preparation and Characterization of an Azide-Alkyne Cycloaddition Based Self-Healing System via a Semiencapsulation Method. *RSC Adv.* **2015**, *5* (112), 92480–92489.
- (35) Huang, H.; Chung, J. Y.; Nolte, A. J.; Stafford, C. M. Characterizing Polymer Brushes via Surface Wrinkling. *Chem. Mater.* **2007**, 19 (26), 6555–6560.
- (36) Ohno, K.; Morinaga, T.; Koh, K.; Tsujii, Y.; Fukuda, T. Synthesis of Monodisperse Silica Particles Coated with Well-Defined, High-Density Polymer Brushes by Surface-Initiated Atom Transfer Radical Polymerization. *Macromolecules* **2005**, 38 (6), 2137–2142.
- (37) Jeyaprakash, J. D.; Samuel, S.; Dhamodharan, R.; Rühe, J. Polymer Brushes via ATRP: Role of Activator and Deactivator in the Surface-Initiated ATRP of Styrene on Planar Substrates. *Macromol. Rapid Commun.* **2002**, 23 (4), 277–281.
- (38) Patil, R. R.; Turgman-Cohen, S.; Šrogl, J.; Kiserow, D.; Genzer, J. Direct Measurement of Molecular Weight and Grafting Density by Controlled and Quantitative Degrafting of Surface-Anchored Poly-(Methyl Methacrylate). ACS Macro Lett. 2015, 4 (2), 251–254.
- (39) Petre, D. G.; Nadar, R.; Tu, Y.; Paknahad, A.; Wilson, D. A.; Leeuwenburgh, S. C. G. Thermoresponsive Brushes Facilitate Effective Reinforcement of Calcium Phosphate Cements. *ACS Appl. Mater. Interfaces* **2019**, *11* (30), 26690–26703.
- (40) Duque-Sánchez, L.; Brack, N.; Postma, A.; Pigram, P. J.; Meagher, L. Optimisation of Grafting of Low Fouling Polymers from Three-Dimensional Scaffolds: Via Surface-Initiated Cu(0) Mediated Polymerisation. *J. Mater. Chem. B* **2018**, *6* (37), 5896–5909.
- (41) Micciulla, S.; Gerelli, Y.; Campbell, R. A.; Schneck, E. A Versatile Method for the Distance-Dependent Structural Characterization of Interacting Soft Interfaces by Neutron Reflectometry. *Langmuir* **2018**, *34* (3), 789–800.
- (42) Julthongpiput, D.; LeMieux, M.; Tsukruk, V. V. Micromechanical Properties of Glassy and Rubbery Polymer Brush Layers as Probed by Atomic Force Microscopy. *Polymer (Guildf)* **2003**, *44* (16), 4557–4562.